

Effect of Shape and Slenderness Ratio on the Behavior of Laterally Loaded Piles

Jasim M. Abbas
Department of Civil and Structural
Engineering, University
Kebangsaan Malaysia
e-mail: jasimalshamary@yahoo.com

Qassun S. Mohammed Shafiqu
Department of Civil Engineering,
Nahrain University, Iraq

Mohd R. Taha
Department of Civil and Structural
Engineering, University
Kebangsaan Malaysia

Abstract

In case of piles subjected to lateral loading, the failure mechanisms of short pile under lateral loads are different from that of long pile case. The lateral load capacity of pile is limited in lateral deformation of the pile that effected directly on the contact surface area. The results of the 3D finite element analysis for the problem of a single pile under lateral loadings are presented in this paper. The effect of pile shape for both circular and square cross-section on pile response was investigated. Also the influence of slenderness ratio L/B on the pile deformation was discussed in this study. Linear elastic model was used for modeling the piles. Mohr-Coulomb model was used to simulate the surrounded soil. The pile – soil interaction composed of 16-node interface elements. A good correlation between the experiments and the analysis was observed in validation example. It was found that the pile response is affected by the amount of loading, the pile cross – sectional shape and pile slenderness ratio. The lateral resisting of pile increase in proportioned to the square shape of the pile. In both pile shape, a short pile ($L/B = 8.3$) gave a small amount of lateral tip deflection than the long pile with a slenderness ratio more than 8.3 for the same amount of loading. Also, the negative base deflection is high for short pile and reduces to zero for long pile.

Keywords: single pile, shape effect, lateral load, Mohr-Coulomb, 3D FEM

1. Introduction

Pile defined as a structural member almost from concrete used to carry applied load from the superstructure to deep strong stratum as well as reinforced the soil. The piles penetration depth (length) depends on the magnitude of applied load and type of soil. In case of piles subject to

lateral loading, the failure mechanisms of short piles under lateral loads are different with long piles case.

The lateral resistance of pile foundations is often important in the design of structures that may be subjected to earthquakes, high winds, wave action, and ship impacts [8]. Vertical piles resist lateral loads or moments by deflecting laterally until the necessary reaction in the surrounding soil is mobilized [11]. In the design of pile subjected to lateral load, ultimate lateral resistance of a pile is required that satisfy two criteria [9, 10], (1) a pile should be safe against ultimate failure; and (2) normal deflection at working loads should be within the permissible limit.

Lately both industry and researchers have begun to explore the advantages of using other cross-sectional shapes rather than the traditional circular pile. These shapes have included solid concrete octagonal and square piles [4].

The finite element method is most widely used to perform the analysis of piles under lateral loads. As reported literature [10] the first attempts to study the lateral behavior of piles included two-dimensional finite element models in the horizontal plane. Many investigations occurring to study the behavior of pile under lateral load [5, 6, 7, 11, 12]. Thus the analyses of laterally loaded piles are investigated by this approach in this study.

In view of this, the present study will focus on investigating the piles subjected to pure lateral loads through series of finite element simulation and analysis. The influence of applied lateral load magnitude and pile cross-sectional shape on the lateral response of single pile will assess in this paper.

2. Numerical Model

Finite element analyses were performed using the software PLAXIS 3D FOUNDATION version 1.1. According to the finite element

method a continuum was divided into number of (volume) elements. Each element consists of a number of nodes. Each node has a number of

degrees of freedom that correspond to discrete values of the unknowns in the boundary value problem to be solved.

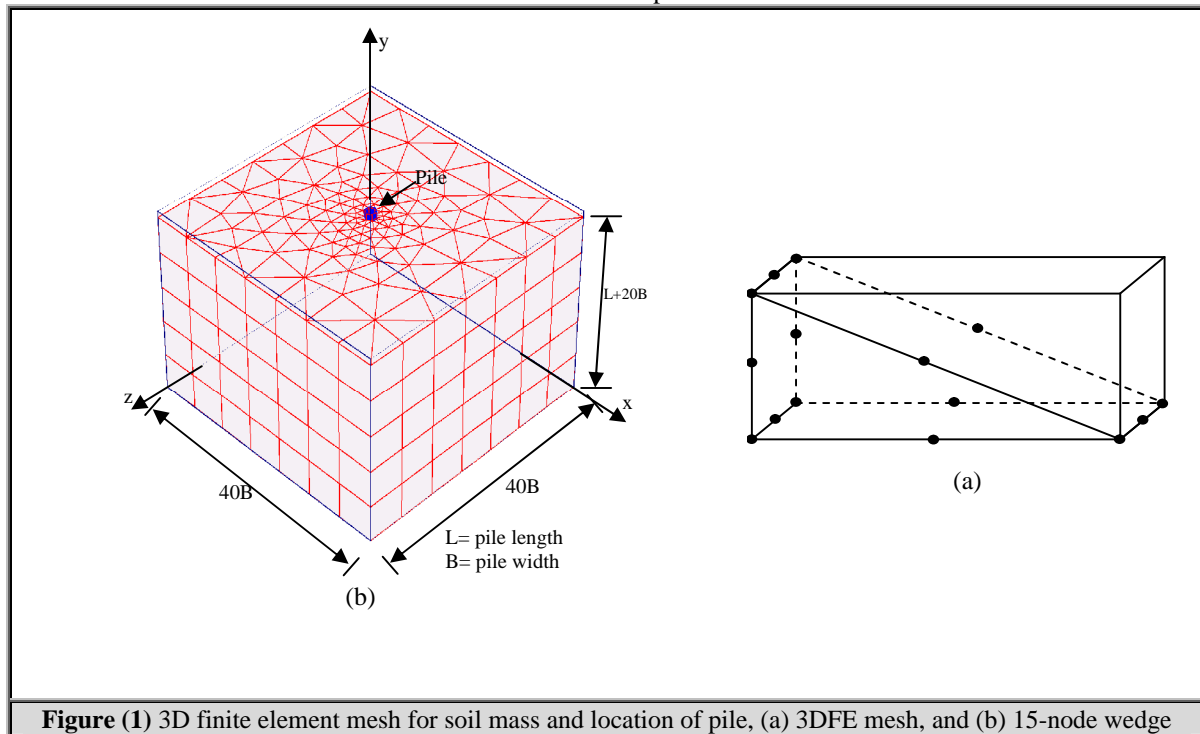


Figure (1) 3D finite element mesh for soil mass and location of pile, (a) 3DFE mesh, and (b) 15-node wedge

2.1 Mesh Generation

In order to perform the finite element calculations, the geometry has to be divided into elements. A composition of finite elements is called a finite element mesh. The basic soil elements of a 3D finite element mesh are represented by the 15-node wedge elements as shown in Figure 1. These elements are generated from the 6-node triangular elements. The 15-node wedge element is composed of 6-node triangles in horizontal direction and 8-node quadrilaterals in vertical direction. According to last study [5, 6] the soil mass dimension depends on the pile diameter and length. The width of soil mass is taken as $40B$, in which, B is the pile diameter or pile width. The soil mass effect on the pile response is diminishing for the width more than $40B$. The height of soil mass is $L+20B$, in which, L is the length of pile.

2.2 Pile Model (linear-elastic model)

This model represents Hooke's law of isotropic linear elasticity used for modeling the stress-strain relationship of the pile material. The model involves two elastic stiffness parameters, namely Young's modulus, E , and Poisson's ratio,

ν , as shown in Figure 2. It is primarily used for modeling of stiff structural member for example piles in the soil [2].

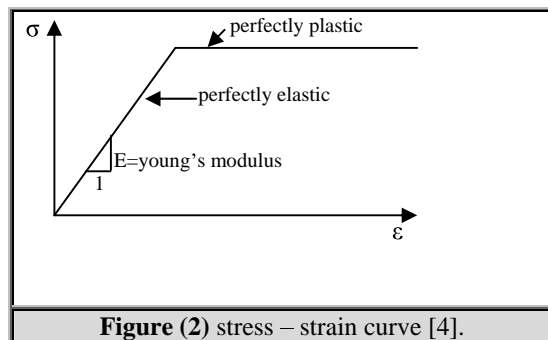


Figure (2) stress – strain curve [4].

Hooke's law can be given by the equation 1. Two parameters are used in this model, the effective Young's modulus, E' , and the effective Poisson's ratio, ν' .

$$\begin{bmatrix} \sigma'_{xx} \\ \sigma'_{yy} \\ \sigma'_{zz} \\ \sigma'_{xy} \\ \sigma'_{yz} \\ \sigma'_{zx} \end{bmatrix} = \frac{E'}{(1-2\nu')(1+\nu')} \begin{bmatrix} 1-\nu' & \nu' & \nu' & 0 & 0 & 0 \\ \nu' & 1-\nu' & \nu' & 0 & 0 & 0 \\ \nu' & \nu' & 1-\nu' & 0 & 0 & 0 \\ 0 & 0 & 0 & \frac{1}{2} & -\nu' & 0 \\ 0 & 0 & 0 & -\nu' & \frac{1}{2} & 0 \\ 0 & 0 & 0 & 0 & -\nu' & \frac{1}{2} \end{bmatrix} \begin{bmatrix} \epsilon'_{xx} \\ \epsilon'_{yy} \\ \epsilon'_{zz} \\ \gamma'_{xy} \\ \gamma'_{yz} \\ \gamma'_{zx} \end{bmatrix} \quad \mathbf{1}$$

The relationship between Young's modulus E and other stiffness moduli, such as the shear modulus G , the bulk modulus K , and constrained modulus M , is given by:

$$G = \frac{E}{2(1+\nu)} \quad 2$$

$$K = \frac{E}{3(1-2\nu)} \quad 3$$

$$M = \frac{(1-\nu)E}{(1-2\nu)(1+\nu)} \quad 4$$

2.3 Soil Model (Mohr-Coulomb Model)

This elasto-plastic model is based on soil parameters that are known in most practical situations. The Mohr-Coulomb model is used to compute realistic bearing capacities and collapse loads of footings, as well as other applications in which the failure behavior of the soil plays a dominant role. The model involves two main parameters, namely the cohesion intercept, c and the friction angle, ϕ . In addition to three parameters namely Young's modulus, E , Poisson's ratio, ν , and the dilatancy angle, ψ need to calculate the complete $\sigma - \varepsilon$ behavior. Mohr Coulomb's failure surface criteria were shown in Figure 3.

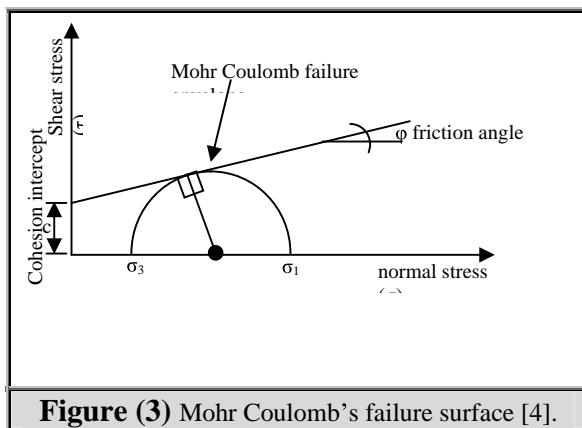


Figure (3) Mohr Coulomb's failure surface [4].

According to Johnson et al. [4] the failure envelope only depend on the principal stresses (σ_1, σ_3), and is independent of the intermediate principle stress (σ_2). When mapped in three-dimensional stress space, Mohr - Coulomb criteria resolved into an irregular hexagonal pyramid. This pyramid forms the failure/yield

envelope, which is turn governs how soil will behave. The material behaves elastically if the stress point lies within the failure envelope. However, if the stress reaches the yield surface the material will undergo a degree of the plastic deformation. In the Mohr - Coulomb model used herein, it is assumed that the soil has a linear elastic relation until failure.

The usual definition of the equation of Mohr-Coulomb surface is :

$$F = \frac{\sigma'_1 + \sigma'_3}{2} \sin \phi' - \frac{\sigma'_1 - \sigma'_3}{2} - c' \cos \phi' \quad 5$$

Which, when rewrite in terms of invariants and Lode angle θ becomes:

$$F = \frac{1}{3} I_1 \sin \phi' + \sqrt{J_2} \left(\cos \theta - \frac{\sin \theta \sin \phi'}{\sqrt{3}} \right) - c' \cos \phi' \quad 6$$

Where:

$$I_1 = \sigma'_x + \sigma'_y + \sigma'_z \quad 7$$

and,

$$J_2 = \frac{1}{6} \left\{ (\sigma'_x - \sigma'_y)^2 + (\sigma'_y - \sigma'_z)^2 + (\sigma'_z - \sigma'_x)^2 \right\} + \tau_{xy}^2 + \tau_{yz}^2 + \tau_{zx}^2 \quad 8$$

2.4 Interface Element

Interfaces are modeled as 16-node interface elements. Interface elements consist of eight pairs of nodes, compatible with the 8-noded quadrilateral side of a soil element. Along degenerated soil elements, interface elements are composed of six node pairs, compatible with the triangular side of the degenerated soil element. Each interface has a 'virtual thickness' assigned to it which is an imaginary dimension used to obtain the stiffness properties of the interface. The virtual thickness is defined as the virtual thickness factor times the average element size. The average element size is determined by the global coarseness setting for the 2D mesh generation. The default value of the virtual thickness factor that is used in this study is 0.1. The stiffness matrix for quadrilateral interface elements is obtained by means of Gaussian integration using 3x3 integration points. The position of these integration points (or stress points) is chosen such that the numerical integration is exact for linear stress distributions.

The 8-node quadrilateral elements provide a second-order interpolation of displacements. Quadrilateral elements have two local coordinates (ξ and η)

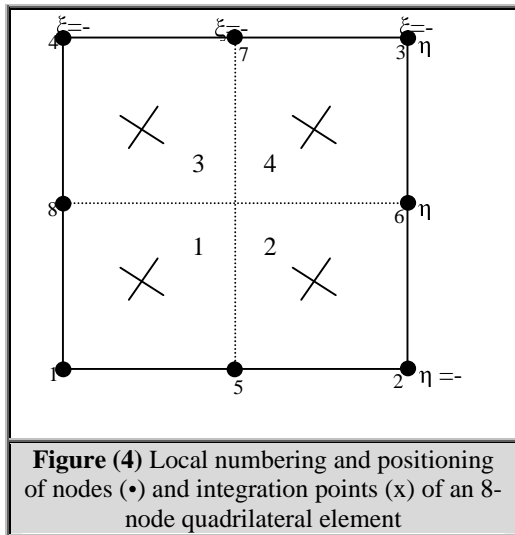


Figure (4) Local numbering and positioning of nodes (•) and integration points (x) of an 8-node quadrilateral element

medium dense cemented silty sand layer to a depth 3m. This is underlain by medium dense to very dense silty sand with cemented lumps to the bottom of the borehole. The all properties of soil were in the both cases listed in Table (1). Ground water was not encountered within the depth of the borehole. The same load sequence was apply on the pile after complete the whole geotechnical model for vertical and lateral pile tests.

In conclusion, the comparison between the finite element simulation and the reported in lateral data is shown in Figure 5. The piles were deflecting not in the same magnitude at the field test due to the variability of soil properties. Also the numerical simulation is reasonably accurate for the problem of laterally loaded piles and pile – soil interaction over a wide range of deformation for 3m and 5m piles long. The pile with length 5m is highly resistance the lateral load from the second pile length value.

3. Validation of Numerical Models

The lateral load – deflection response of bored piles in cemented sand was examined by field test on single pile under lateral load was reported by [3]. All piles were 0.3m in diameter and had a length of 3m or 5m. A site was selected in Kuwait. The surface soil to depth of 3.5m was characterized as having both component of shear strength, c and ϕ . The soil profile consists of a

Table (1) Geotechnical properties of the soil layers for case

Parameter	Name	medium dense cemented silty sand layer	medium dense to very dense silty sand with cemented lumps	Pile	Unit
Unsaturated soil weight	γ_{unsat}	18	19	25	kN/m ³
Saturated soil weight	γ_{sat}	18	19	-	kN/m ³
Young's modulus	E	1.300E+04	1.300E+04	2E+09	kPa
Poisson's constant	ν	0.3	0.3	0.15	-
Cohesion	c	20	1	-	kPa
Friction angle	ϕ	35	45	-	-

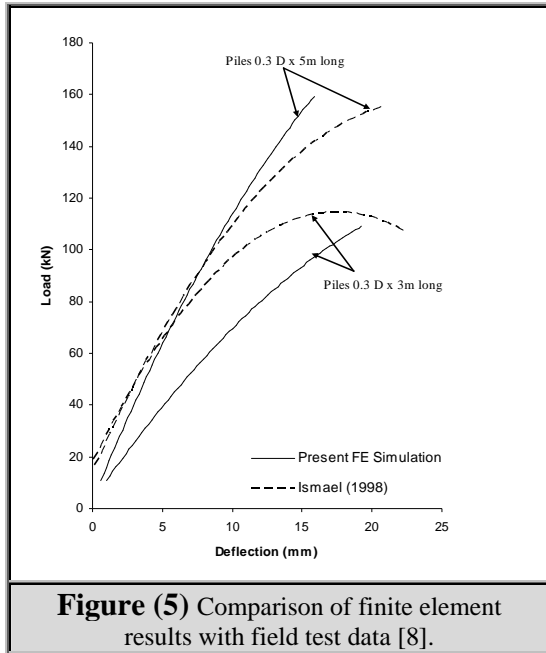


Figure (5) Comparison of finite element results with field test data [8].

4. Results and Discussion

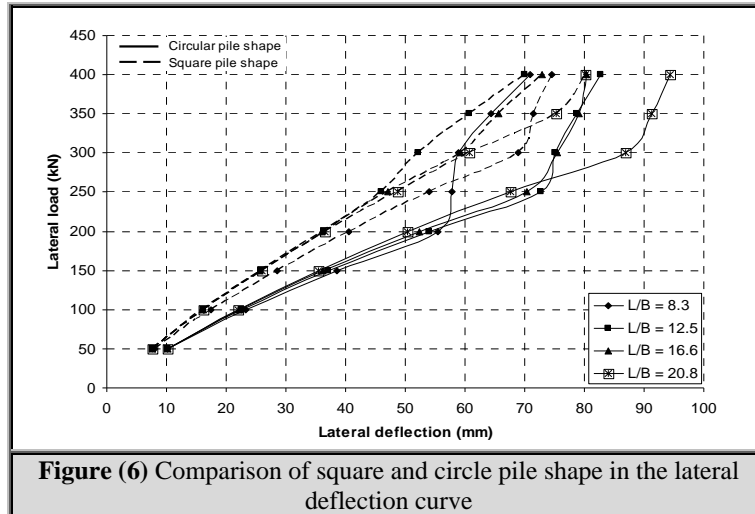
Pile behavior mainly depends on the interaction between pile material and the soil media when piles are subjected to lateral load. This study includes: (1) the magnitude of load. Started from the small loading (50 kN) and increased gradually in equal magnitude during the load stages until maximum intensity of (400 kN), (2) pile shape. This factor include the pile cross-sectional shape, first is a ordinary circular shape and the second is a square (rectangular) shape, and (3) the slenderness ratio (L/B). The influence

of these factors are summarized in the following sections

4.1 Material Properties and Dimensions

In this study, circular cast in place test pile was used to simulate the behavior of piles under lateral and vertical load. These piles were embedded into sandy soil in one layer. The test pile properties and dimensions together with soil properties are summarized in Table 2.

parameters	Pile details		Soil details	
	Circle cross-section	Square cross-section	parameters	Values
Size	1200 mm D	1200x1200 mm	Friction angle (ϕ)	30
Length, L	10 m	10 m	Dilation angle (ψ)	0-10
Type of pile	Concrete	Concrete	Unit weight (γ)	18 kN/m ³
Grade of concrete	M25	M25	Young's modulus (E_s)	20 MPa
Young's modulus, E_p	25000 MPa	25000 MPa	Earth pressure Coefficient (k_0)	0.5
Poisson's ratio, ν_s	0.15	0.15	Poisson's ratio (ν)	0.3



All the analysis was performed in two stages. The first stage is to analyze piles that have traditional shape (circular cross section). Then piles of square shape were evaluated in second stage. The lateral behavior of pile in two cross – sectional shape assessed depends on the one layered soil as mentioned before.

This section includes also the load effect on the laterally loading piles with two shapes. The pile of circular cross – section was firstly tested by applied the load in the tip of pile then made a test for square pile cross - section. The loading consists of a small amount of increment which is 50 kN [5, 6] in the beginning of loading stages. The investigation continues to reach a maximum amount of loading that always using in the design of piles when subject to lateral load.

The lateral load – deflection curve of two pile shapes is shown in Figure 6, that detailed the lateral deflection response increased with increased the amount of loading. Pile deflection change depends on the pile load increment. In the first stage of load, the pile response was uniform that mean, the pile deflection improves linearly. But the square pile is more resistant than a circular shape, due to the high contact surface area between the pile and surrounded soil. The pile deflection increase around 60% when the load increase was load by 50 % in the

case of square and circle pile shape. From this comparison can show the square shape pile has a small tip deflection than the circular shape pile in the same load intensity. The square pile shape has a large surface area that improves the lateral soil resistance which decreases the lateral deflection of pile.

The pile deformation due the lateral load is also influenced by pile slenderness ratio (L/B). In Figures 7 the effect of slenderness ratio on the deformation behavior of pile under lateral load show circular and square pile shape: (a) the short pile ($L/B = 8.3$) give a small amount of lateral tip deflection for the same amount of loading than the piles have the slenderness ratio more than 8.3. (b) the deflection along the pile is always in the direction of load (assumed negative). These values changed to positive and pass through zero depending on the slenderness ratio. For the short pile ($L/B = 8.3, 12.5$), the point of inflection is $1/5$ from the base of the pile, while the long pile ($L/B = 16.7, 20.8$), the point position is $3/5$ from the base. This is due to the slenderness of the pile that carry the load along pile length in the case of short piles but the upper part of pile carry applied load in the case of long piles. In generally the pile with square cross section is more resist (low deflection) especially in the case of long pile.

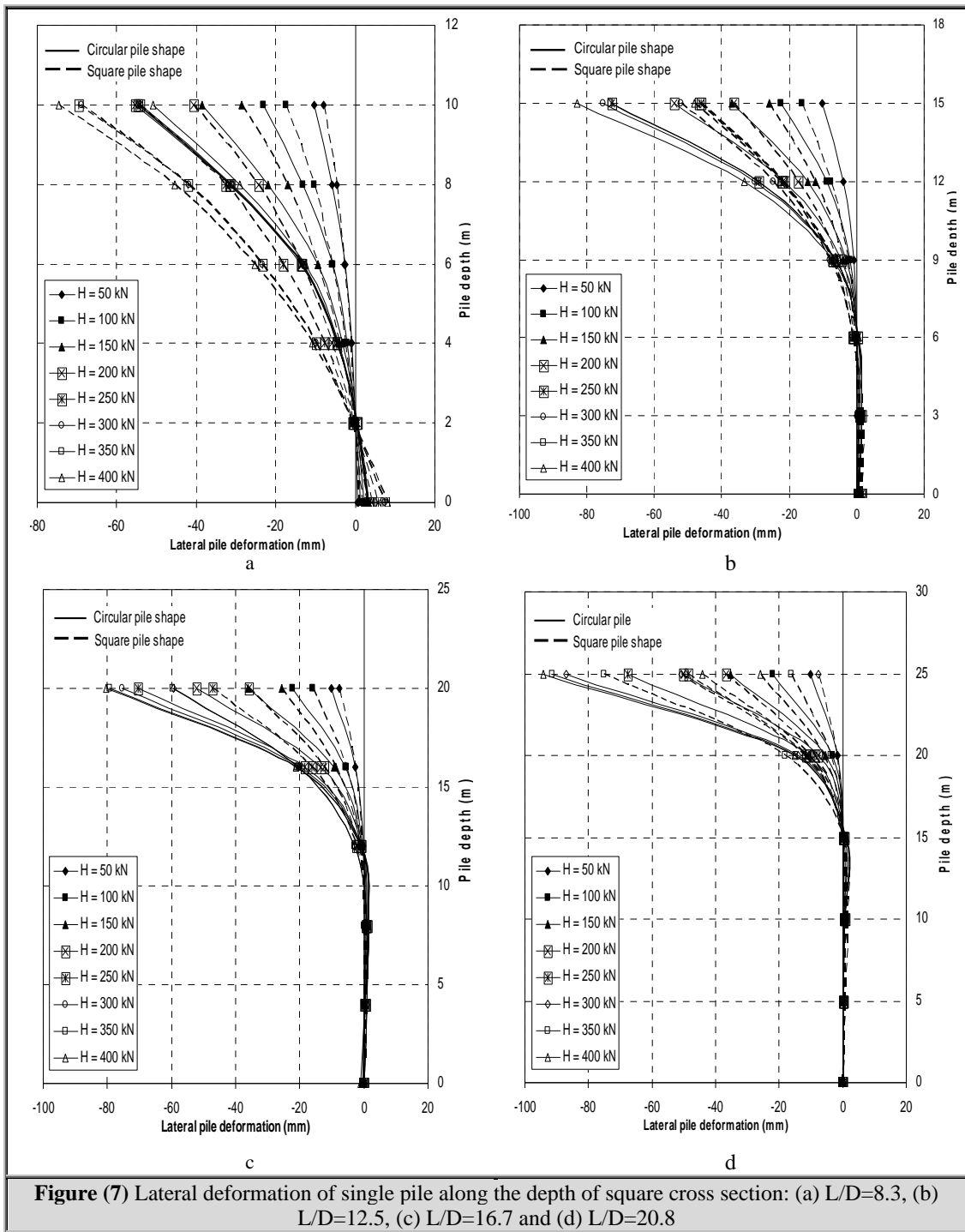


Figure (7) Lateral deformation of single pile along the depth of square cross section: (a) $L/D=8.3$, (b) $L/D=12.5$, (c) $L/D=16.7$ and (d) $L/D=20.8$

In the case of short pile, the pile body tends to rotate around the inflection point and produce a small negative deflection close to the pile base as shown in Figure 7a. The negative deflection occurred in the opposite direction of applied load. The maximum negative deflection occurred

exactly in the base of pile. The circular pile shape has a smaller deflection than the square pile shape because of high pile stiffness in the low loading. While it increased for large amount of loading. These negative deflection reduce to zero when slenderness ratio increased about 50%

and the as shown in Figure 7b with small negative deflection in the case of square pile shape due to high stiffness. For slenderness ratio of 16.7, the maximum negative deflection occurred in the middle part between the base and the inflection point. In the case of long piles, the base deflection is zero and same time the base make a small positive base deflection as shown in Figure 7c. Finally, the negative deflection occurred near to the inflection point. That means, this region is critical closed to inflection point, while the base deflection is zero as shown in Figure 7d.

5. Conclusions

The following conclusions are drawn from the present investigation:

1. The amount of loading is directly affected on deflection and deformation of pile. When the load is increased, the deflection becomes non-uniform. The percentage of pile tip deflection is much more than the percentage of deflection in the pile body.
2. The pile shapes also effect the pile response. The square pile is more resistant the lateral load than a circular shape due to the high contact surface area between the pile and surrounded soil and high bending resistance.
3. The pile deformation that occurs due to lateral load is influenced by pile slenderness ratio (L/B). The short pile (L/B = 8.3) gives a small amount of lateral tip deflection for the same amount of loading than piles having the slenderness ratio more than 8.3. For the short pile (L/B = 8.3, 12.5), the point of inflection is 1/5 from the base of pile. In this case the long piles (L/B = 16.7, 20.8), the point position is 3/5 from the base of pile. In addition the pile body tend to rotate around the inflection point and produce a small negative deflection near to the pile base depend on the magnitude of loads and slenderness ratio.

6. References

- [1] A. Muqtadir and C. S. Desai, "Three-dimensional analysis of a pile-group foundation" . International Journal of Numerical and Analytical Methods Geomechanics Vol.10, pp.41-58, 1986.
- [2] H.G. Poulos, E. H. Davis, "Pile Foundation Analysis and Design". John Wiley & Sons, Inc, United States, 1980.
- [3] J. M. Abbas, Z. H Chik, M. R. Taha, "Single pile simulation and analysis subjected to lateral load" Electronic Journal of Geotechnical Engineering, EJGE. Vol. 13(E2), 2008.
- [4] K. Johnson, P. Lemcke, W. Karunasena, N. Sivakugan, "Modelling the load – deformation response of deep foundation under oblique load" . Environment Modelling and Software, NO. 21, pp.1375-1380, 2006.
- [5] K. M. Rollins, J. D. Lane and T. M. Gerber, "Measured and Computed Lateral Response of a Pile Group in Sand" . Journal of Geotechnical and Geoenvironmental Engineering, Vol. 131, No. 1, pp. 103-114, 2005.
- [6] R. B. J. Brinkgreve and W. Broere, "PLAXIS 3D FOUNDATION - version 1". Netherlands, 2004.
- [7] M. E. Sawwaf, "Lateral Resistance of Single Pile Located Near Geosynthetic Reinforced Slope" Journal of Geotechnical and Geoenvironmental Engineering, Vol. 132, No. 10, pp. 1336-1345, 2006.
- [8] N. F. Ismael, "Lateral loading tests on bored piles in cemented sands". Proceedings of the 3rd International Geotechnical Seminar on Deep Foundation on Bored and Auger Piles, Ghent, Belgium pp.137-144, 1998.
- [9] N. R. Patra and P. J. Pise "Ultimate lateral resistance of pile groups in sand" . Journal of Geotechnical and Geoenvironmental Engineering, ASCE, Vol. 127, No. 6, pp.481-487, 2001.
- [10] S. Karthigeyan, V. V. G. S. T. Ramakrishna and K. Rajagopal, "Influence of vertical load on the lateral response of piles in sand" . Computer and Geotechnics, Vol. 33, pp.121-131, 2006.
- [11] S. Karthigeyan, V. V. G. S. T. Ramakrishna and K. Rajagopal, "Numerical Investigation of the Effect of Vertical Load on the Lateral Response of Piles" . Journal of Geotechnical and Geoenvironmental Engineering, Vol. 133, No. 5, pp. 512-521, 2007.
- [12] Z. Yang, and B. Jeremi?, "Study of Soil Layering Effects on Lateral Loading Behavior of Piles" . Journal of Geotec Geoenvironmental Engineering, Vol. 131, No. 6, pp.762-770, 2005.

تأثير الشكل ونسبة الرشاقة على تصرف الركائز المحملة بقوى جانبي

جاسم محمد عباس^١، قاسيون سعدالدين محمد شفيق^٢، محمد ربحان طه^٣، زمري جيكا^٤
أقسام الهندسة المدنية والاثنائية، الجامعة الوطنية الماليزية، ماليزيا
قسم الهندسة المدنية، جامعة النهرين، العراق

الخلاصة

في حالة الركائز المحملة بالقوة الجانبية فان ميكانيكية الفشل للركائز القصيرة تحت القوى الجانبية تختلف منها في حالة الركائز الطويلة. مقدار تحمل الركيزة للقوى الجانبية محددة بالازاحات الجانبية لها والتي تؤثر مباشرة على المساحة السطحية لمنطقة التلامس. نتائج التحليل ثلاثي الابعاد بطريقة العناصر المحددة لمسألة الركيزة تحت القوى الجانبية قد بحثت في هذه الدراسة. ان تأثير شكل المقطع الدائري والمربع للركيزة على تصرفها قد تم بحثها. اضافة الى تأثير نسبة الرشاقة (L/B) على ازاحات الركيزة قد نوقشت في هذه الدراسة. النموذج اللدن الخطي تم استخدامها لتمثيل الركائز. كما ان نموذج Mohr-Coulomb قد تم استخدامها لتمثيل تصرف التربة المحيطة. منطقة التلامس بين الركيزة والتربة تضمنت عناصر التلامس ذات الستة عشرة عقدة. مقارنة جيدة وجدت بين النتائج العملية والنظرية في مسألة التدقيق. وجد ايضا بان تصرف الركيزة تتاثر بكمية القوى المسلطة، شكل مقطع الركيزة وايضا نسبة الرشاقة. وان المقاومة الجانبية للركيزة تزداد بشكل متناسب مع المقطع المربع للركيزة. وفي حالة كلا المقطعين فان الركيزة القصيرة ذات الابعاد ($L/B=8.3$) اعطت قيم صغيرة للازاحة الجانبية في قمة الركيزة مقارنة مع الركيزة الطويلة مع نسبة رشاقة زادت عن 8.3 لنفس قيمة القوة المسلطة. ايضا، الازاحة السالبة في قاعدة الركيزة كانت عالية في حالة الركيزة القصيرة وتقل الى ان تصل الى الصفر في حالة الركيزة الطويلة.

This document was created with Win2PDF available at <http://www.daneprairie.com>.
The unregistered version of Win2PDF is for evaluation or non-commercial use only.